Supplement of Biogeosciences, 20, 3229–3247, 2023
https://doi.org/10.5194/bg-20-3229-2023-supplement

Biogeosciences Open Access EGU

Supplement of

Seasonal variability of nitrous oxide concentrations and emissions in a temperate estuary

Gesa Schulz et al.

Correspondence to: Gesa Schulz (gesa.schulz@hereon.de)

Table S1: Applied oxygen correction for each cruise: The corrections were made using the salinity corrected optode measurements from the FerryBox (O2) in comparison with Winkler titrations. Changes in oxygen corrections arose due to several optode changes in the time period from 2017 to 2022.

Cruise	Correction	Number of Winkler titrations	R^2
2017/08	+24.05 ± 1.52	7	
2019/06	+35.19 ± 5.97	9	
2019/07	+35.19 ± 5.97	9	
2020/06	-2.38	19	0.99
2020/09	-2.38	19	0.99
2021/03	0.97 × O2 + 43.91	22	0.94
2021/05	1.12 × O2 + 13.41	36	0.97
2021/07	1.12 × O2 + 13.41	36	0.97
2022/03	1.12 × O2 + 13.41	36	0.97

Table S2: Calculated average N_2O saturation, sea-to-air fluxes calculated after different parametrizations and atmospheric N_2O dry mole fractions during our cruises

Campaign Dates	Average saturation (%)	N_2O Flux densities (µmol m^{-2} d^{-1})								
		Nightingale et al. (2000)			Wanninkhof (1992)			Clark et al. (1995)		
		In-situ wind	Annual wind	Seasonal wind	In-situ wind	Annual wind	Seasonal wind	In-situ wind	Annual wind	Seasonal wind
28.-29.04.15	160.8 ± 37.9	20.9 ± 13.3	9.2 ± 5.9	11.5 ± 7.3	24.3 ± 15.4	9.8 ± 6.2	12.6 ± 8.0	21.6 ± 13.7	10.4 ± 6.6	12.6 ± 8.0
02.-04.06.15	203.8 ± 112.7	16.6 ± 18.2	14.9 ± 16.3	15.4 ± 16.9	17.8 ± 19.5	15.8 ± 17.2	16.4 ± 18.0	18.4 ± 20.1	16.8 ± 18.4	17.3 ± 19.0
01.-02.08.17	221.0 ± 106.5	10.9 ± 9.7	17.3 ± 15.4	18.1 ± 16.2	10.7 ± 9.6	18.3 ± 16.3	19.3 ± 17.2	13.7 ± 12.2	19.5 ± 17.4	20.3 ± 18.1
04.-05.06.19	192.6 ± 66.0	10.1 ± 7.3	13.4 ± 9.7	13.9 ± 10.0	10.3 ± 7.4	14.2 ± 10.2	14.8 ± 10.7	12.1 ± 8.7	15.1 ± 10.9	15.6 ± 11.3
30.07.-01.08.19	232.5 ± 155.3	15.0 ± 17.9	18.3 ± 21.8	19.9 ± 23.7	15.4 ± 18.4	19.3 ± 23.1	21.3 ± 25.4	17.6 ± 21.0	20.6 ± 24.6	22.1 ± 26.4
19.-20.06.20	193.9 ± 74.1	19.4 ± 15.6	13.3 ± 10.8	13.8 ± 11.2	21.5 ± 17.3	14.1 ± 11.4	14.7 ± 11.9	20.8 ± 16.7	15.1 ± 12.1	15.5 ± 12.5
09.-11.09.20	160.5 ± 53.6	13.1 ± 11.8	8.7 ± 7.9	11.4 ± 10.3	14.6 ± 13.2	9.2 ± 8.4	12.5 ± 11.3	14.0 ± 12.6	9.9 ± 8.9	12.4 ± 11.2
10.-12.03.21	242.5 ± 141.6	80.1 ± 80.5	23.2 ± 23.3	37.0 ± 37.1	96.3 ± 96.8	24.6 ± 24.7	41.4 ± 41.6	81.7 ± 82.1	26.2 ± 26.3	39.3 ± 39.4
04.-05.05.21	145.6 ± 28.8	33.5 ± 21.2	7.1 ± 4.5	7.8 ± 4.9	41.2 ± 26.0	7.5 ± 4.7	8.4 ± 5.3	34.1 ± 21.5	8.0 ± 5.1	8.7 ± 5.5
27.-28.07.21	172.6 ± 37.2	12.4 ± 6.5	10.4 ± 5.4	11.3 ± 5.9	13.4 ± 7.0	11.0 ± 5.7	12.1 ± 6.3	13.6 ± 7.1	11.7 ± 6.1	12.5 ± 6.6
01.-02.03.22	196.5 ± 47.0	6.8 ± 3.4	15.6 ± 7.8	24.8 ± 12.4	6.3 ± 3.1	16.5 ± 8.2	27.8 ± 13.9	9.7 ± 4.8	17.6 ± 8.8	26.3 ± 13.2

Table S3: Areas for different section of the Elbe estuary used for N_2O emission estimates

Section	Stream kilometer (km)	Area (km²)
Limnic	585 – 615	8
Port	615 – 632	22
Oligohaline	632 – 704	162
Mesohaline	704 – 727	110
Polyhaline	727 – 750	148
Total	585 – 750	450

Table S4: Annual DIN and TN loads calculated according to Pätsch and Lenhart (2011) from 2015 to 2021. We used publicly available data provided by FGG Elbe (2022). For 2022, data is not publicly available yet.

Year	DIN (Gg yr^{-1})	TN (Gg yr^{-1})
2015	41.4	59.4
2016	47.5	60.3
2017	53.9	70.2
2018	40.7	51.1
2019	36.7	43.1
2020	36.8	44.5
2021	55.0	63.0
Mean	44.6	55.0

Table S5: Calculated average seasonal DIN and TN loads from 2015 to 2021

Season	Months	DIN (g d^{-1})	TN (g d^{-1})
Winter	March	$2.91 \times 10^8 \pm 1.05 \times 10^8$	$3.34 \times 10^8 \pm 9.40 \times 10^7$
Spring	April and May	$1.17 \times 10^8 \pm 6.24 \times 10^7$	$1.58 \times 10^8 \pm 7.62 \times 10^7$
Summer	June and July	$5.03 \times 10^7 \pm 3.36 \times 10^7$	$7.37 \times 10^7 \pm 3.99 \times 10^7$
Late summer	August and September	$4.33 \times 10^7 \pm 2.69 \times 10^7$	$6.25 \times 10^7 \pm 3.58 \times 10^7$

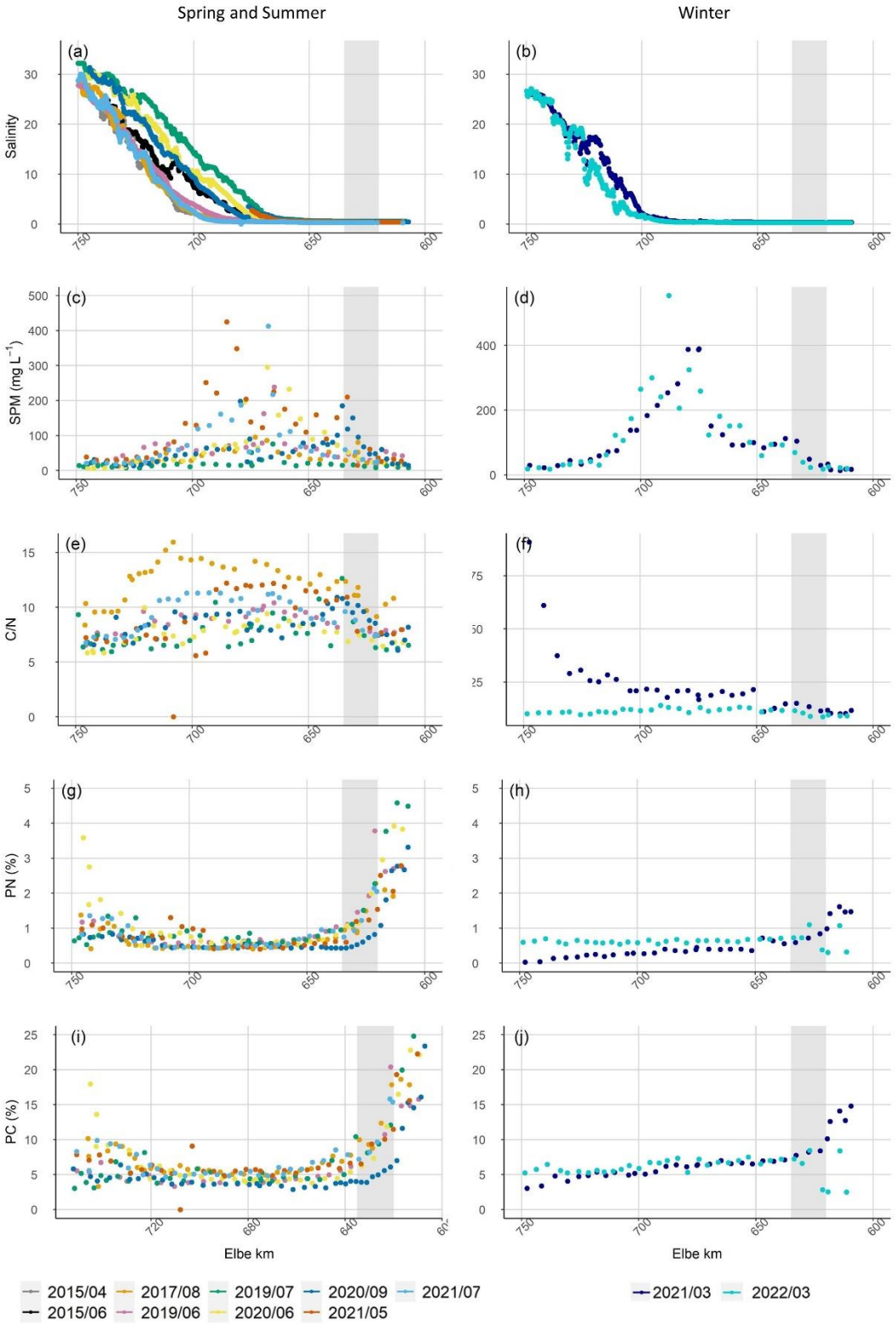

Figure S1: Salinity along the Elbe estuary (a) in spring/summer and (b) in winter. Suspended particulate matter (SPM) concentration in (mg L^{-1}) along the Elbe estuary in (c) spring/summer and (d) in winter. Particulate carbon to nitrogen ratio (C/N) along the Elbe estuary in (e) in spring/summer and (f) in winter. Particulate nitrogen (PN) content in (%) in (g) spring/summer and (h) winter. Particulate carbon (PC) content in (%) in (i) spring/summer and (j) winter. All values are potted against stream kilometers. The Hamburg port region is shown with a gray background. C/N ratios were measured with an Elemental Analyzer (Eurovector EA 3000) calibrated against a certified acetanilide standard (IVA Analysentechnik, Germany). The standard deviation was 0.05% and 0.005% for carbon and nitrogen respectively. Please note that there are no data for the suspended particulate matter composition in 2015.

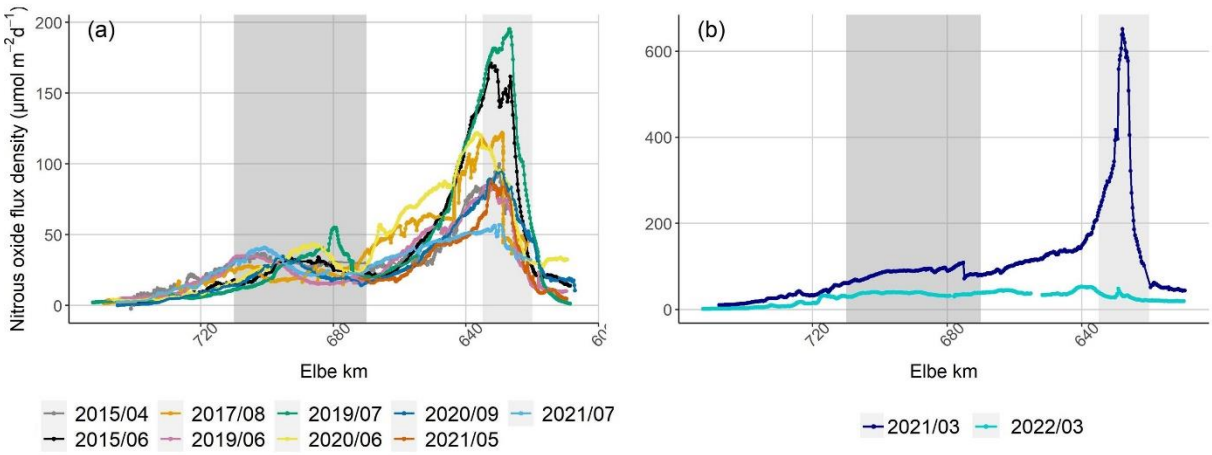

Figure S2: Nitrous oxide flux density along the Elbe estuary calculated after Borges et al. (2004) and in-situ wind speeds (a) in spring and summer, (b) in winter. Light grey shading denotes the Hamburg Port region, dark grey shading the typical position of the maximum turbidity zone (MTZ, Bergemann, 2004). Note the difference in Y-axis scales for the plots.

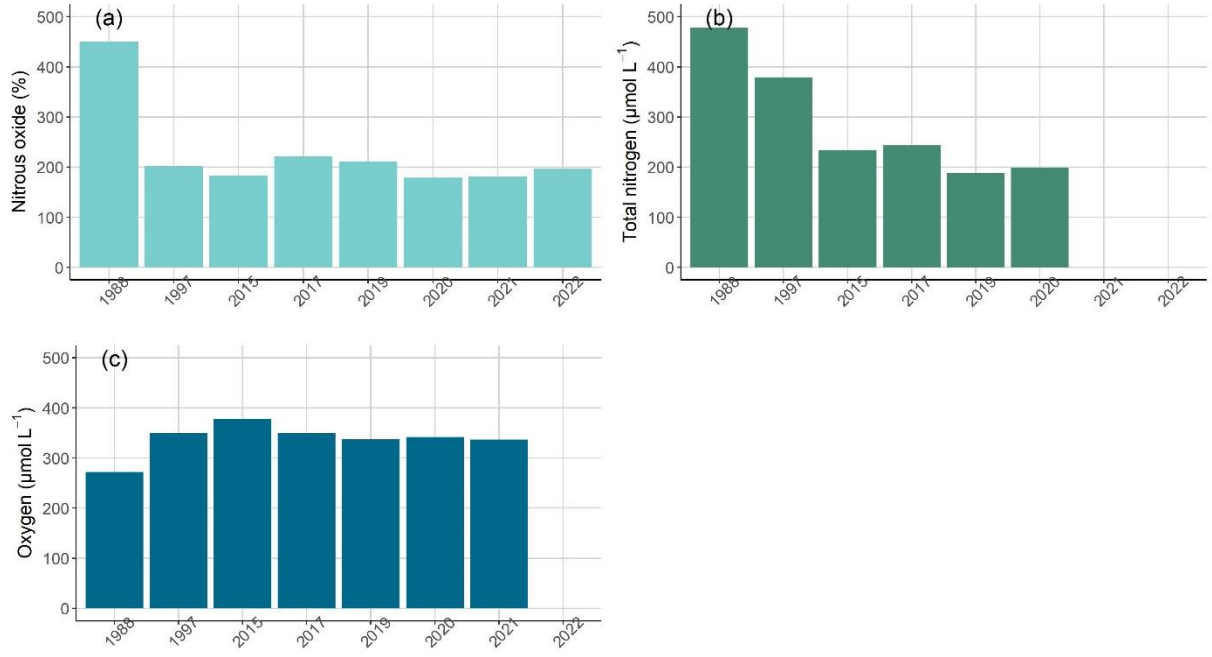

Figure S3: (a) Comparison of average N_2O saturation transect measurements with previous research from the Elbe Estuary, (b) the total nitrogen concentration and (c) oxygen concentration. Average annual oxygen concentration and total nitrogen concentration are shown for the station Zollenspieker at the beginning of the estuary (stream kilometer 598.7) and publicly available (Das Fachinfomrationssystem (FIS) der FGG Elbe, 2022).Values for 2022 and total nitrogen concentration for 2021 are not presented as the data is not publicly available yet.

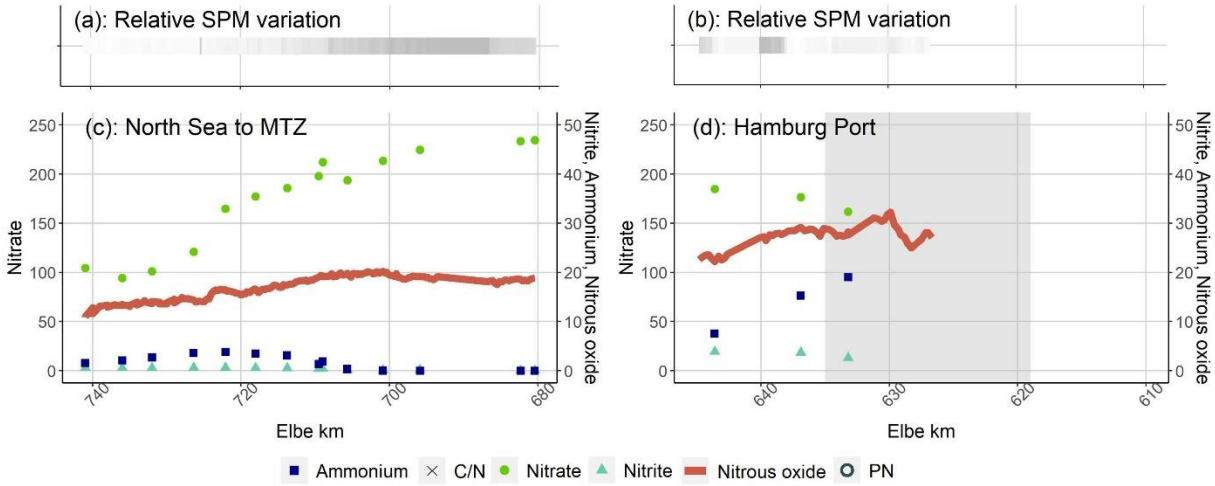

Figure S4: Succession of N-bearing substances coming from the North Sea and in the Port of Hamburg in April 2015: Relative change of SPM concentrations (a) from the North Sea and (b) in the Port of Hamburg. Nitrate in µmol L^{-1}, nitrite in µmol L^{-1}, ammonium in µmol L^{-1} and nitrous oxide concentrations in nmol L^{-1} plotted against stream kilometers (c) from the North Sea and (d) in the Port of Hamburg. The grey area in (d) and (f) shows the position of the Port of Hamburg.

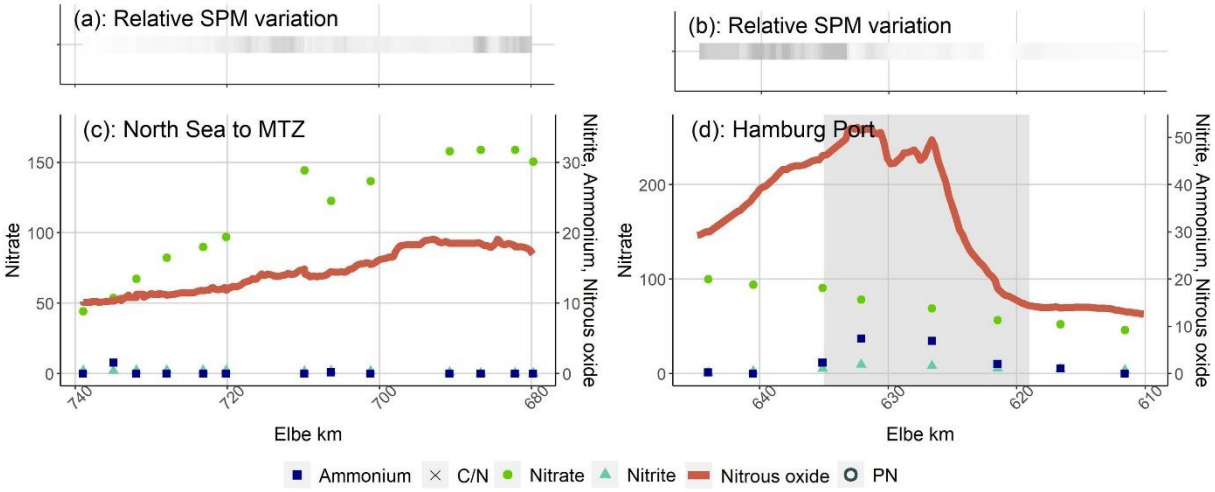

Figure S5: Succession of N-bearing substances coming from the North Sea and in the Port of Hamburg in June 2015: Relative change of SPM concentrations (a) from the North Sea and (b) in the Port of Hamburg. Nitrate in µmol L^{-1}, nitrite in µmol L^{-1}, ammonium in µmol L^{-1} and nitrous oxide concentrations in nmol L^{-1} plotted against stream kilometers (c) from the North Sea and (d) in the Port of Hamburg. The grey area in (d) and (f) shows the position of the Port of Hamburg.

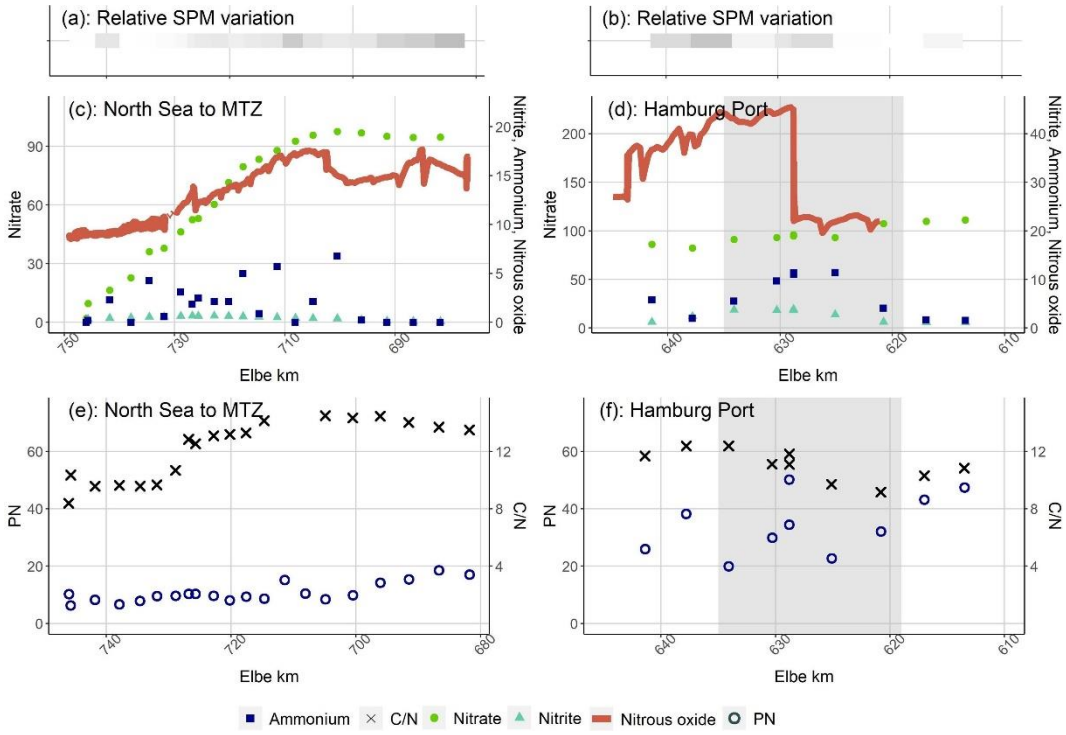

Figure S6: Succession of N-bearing substances coming from the North Sea and in the Port of Hamburg in August 2017: Relative change of SPM concentrations (a) from the North Sea and (b) in the Port of Hamburg. Nitrate in µmol L^{-1}, nitrite in µmol L^{-1}, ammonium in µmol L^{-1} and nitrous oxide concentrations in nmol L^{-1} plotted against stream kilometers (c) from the North Sea and (d) in the Port of Hamburg. Particulate nitrogen concentrations in µmol L^{-1} and C/N values plotted against stream kilometers (e) from the North Sea and (f) in the Port of Hamburg. The grey area in (d) and (f) shows the position of the Port of Hamburg.

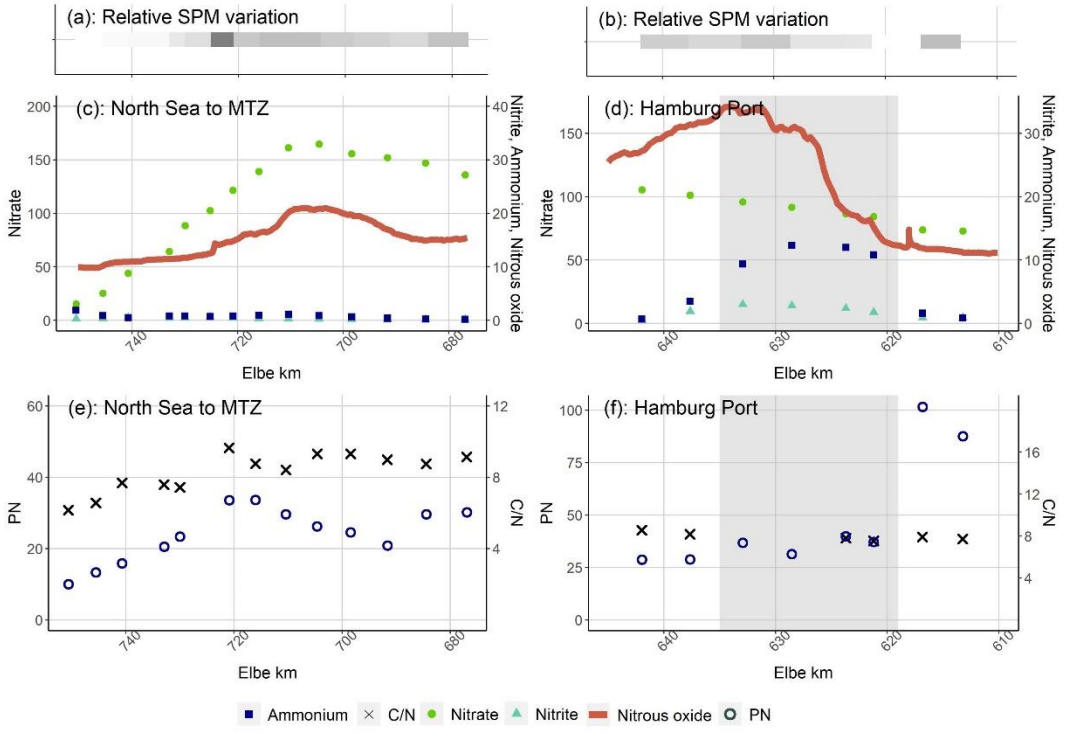

Figure S7: Succession of N-bearing substances coming from the North Sea and in the Port of Hamburg in June 2019: Relative change of SPM concentrations (a) from the North Sea and (b) in the Port of Hamburg. Nitrate in µmol L^{-1}, nitrite in µmol L^{-1}, ammonium in µmol L^{-1} and nitrous oxide concentrations in nmol L^{-1} plotted against stream kilometers (c) from the North Sea and (d) in the Port of Hamburg. Particulate nitrogen concentrations in µmol L^{-1} and C/N values plotted against stream kilometers (e) from the North Sea and (f) in the Port of Hamburg. The grey area in (d) and (f) shows the position of the Port of Hamburg.

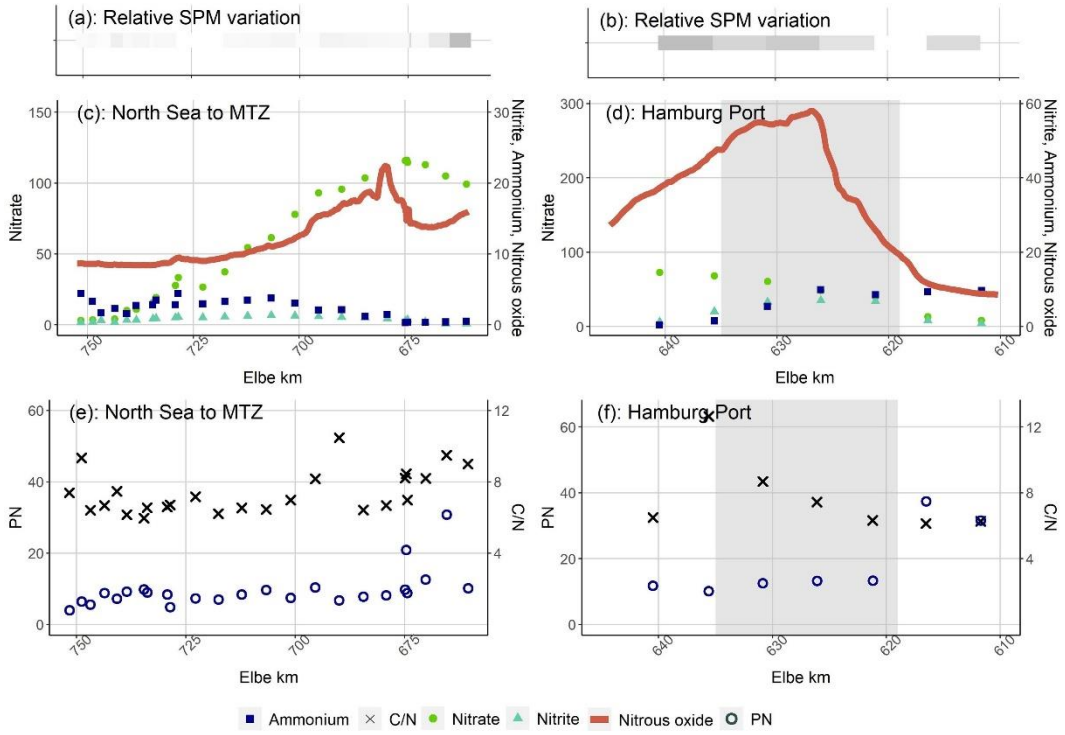

Figure S8: Succession of N-bearing substances coming from the North Sea and in the Port of Hamburg in July 2019: Relative change of SPM concentrations (a) from the North Sea and (b) in the Port of Hamburg. Nitrate in µmol L^{-1}, nitrite in µmol L^{-1}, ammonium in µmol L^{-1} and nitrous oxide concentrations in nmol L^{-1} plotted against stream kilometers (c) from the North Sea and (d) in the Port of Hamburg. Particulate nitrogen concentrations in µmol L^{-1} and C/N values plotted against stream kilometers (e) from the North Sea and (f) in the Port of Hamburg. The grey area in (d) and (f) shows the position of the Port of Hamburg.

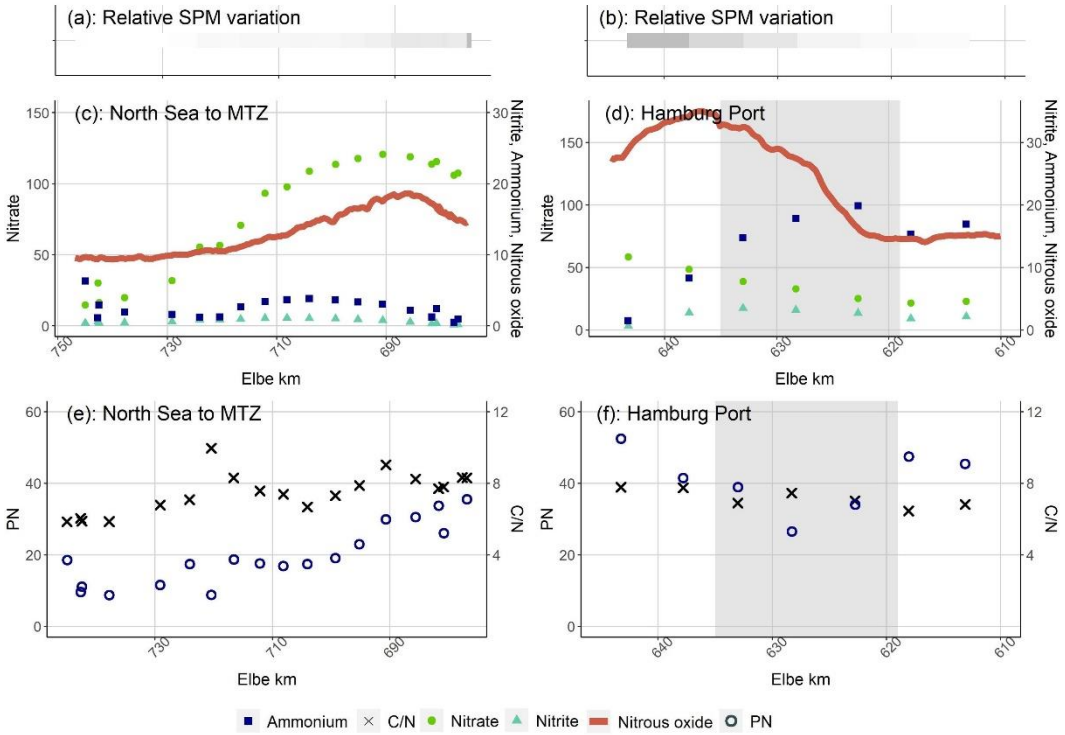

Figure S9: Succession of N-bearing substances coming from the North Sea and in the Port of Hamburg in June 2020: Relative change of SPM concentrations (a) from the North Sea and (b) in the Port of Hamburg. Nitrate in µmol L^{-1}, nitrite in µmol L^{-1}, ammonium in µmol L^{-1} and nitrous oxide concentrations in nmol L^{-1} plotted against stream kilometers (c) from the North Sea and (d) in the Port of Hamburg. Particulate nitrogen concentrations in µmol L^{-1} and C/N values plotted against stream kilometers (e) from the North Sea and (f) in the Port of Hamburg. The grey area in (d) and (f) shows the position of the Port of Hamburg.

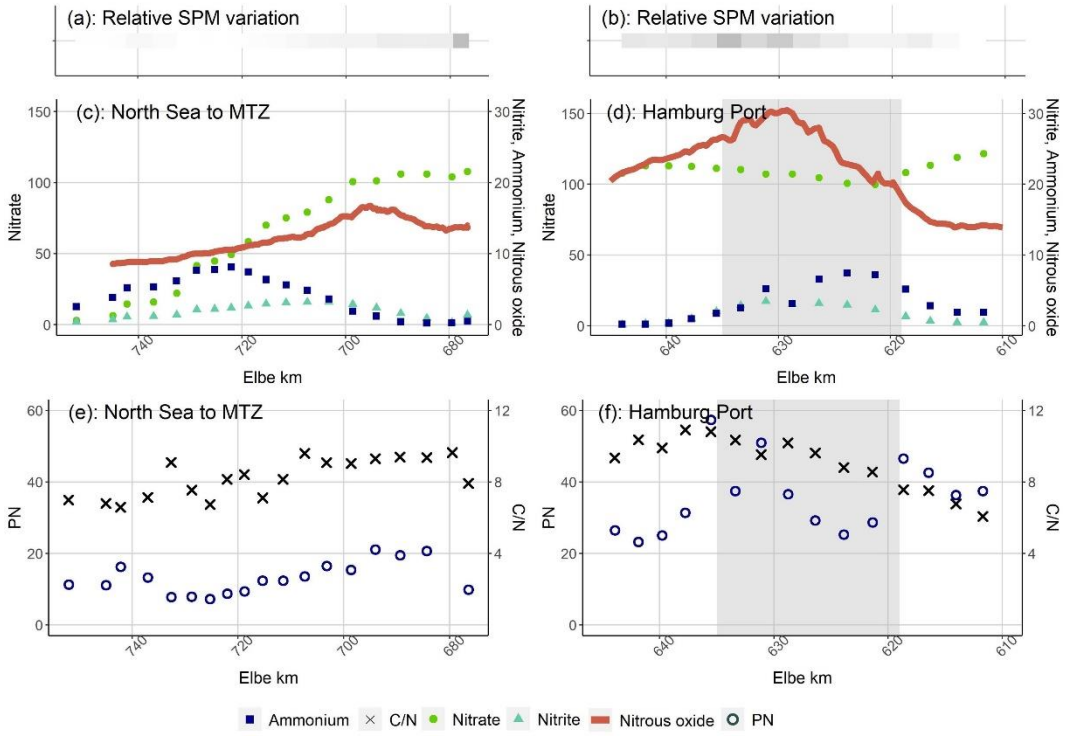

Figure S10: Succession of N-bearing substances coming from the North Sea and in the Port of Hamburg in September 2020: Relative change of SPM concentrations (a) from the North Sea and (b) in the Port of Hamburg. Nitrate in µmol L^{-1}, nitrite in µmol L^{-1}, ammonium in µmol L^{-1} and nitrous oxide concentrations in nmol L^{-1} plotted against stream kilometers (c) from the North Sea and (d) in the Port of Hamburg. Particulate nitrogen concentrations in µmol L^{-1} and C/N values plotted against stream kilometers (e) from the North Sea and (f) in the Port of Hamburg. The grey area in (d) and (f) shows the position of the Port of Hamburg.

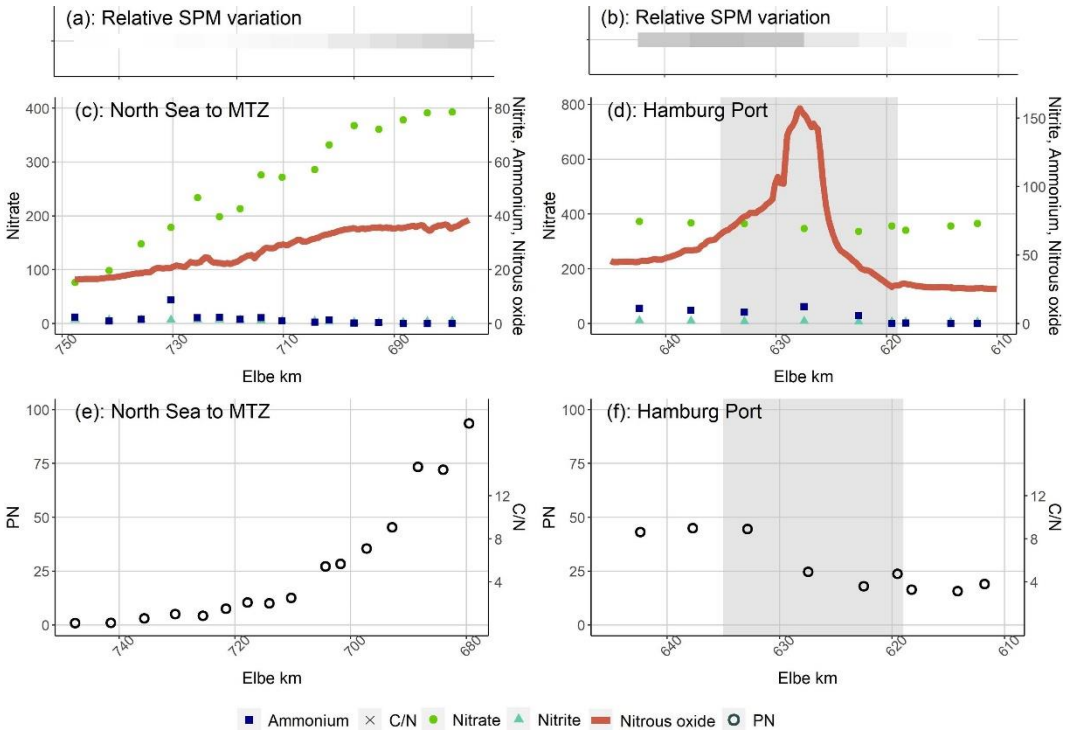

Figure S11: Succession of N-bearing substances coming from the North Sea and in the Port of Hamburg in March 2021: Relative change of SPM concentrations (a) from the North Sea and (b) in the Port of Hamburg. Nitrate in µmol L^{-1}, nitrite in µmol L^{-1}, ammonium in µmol L^{-1} and nitrous oxide concentrations in nmol L^{-1} plotted against stream kilometers (c) from the North Sea and (d) in the Port of Hamburg. Particulate nitrogen concentrations in µmol L^{-1} and C/N values plotted against stream kilometers (e) from the North Sea and (f) in the Port of Hamburg. The grey area in (d) and (f) shows the position of the Port of Hamburg.

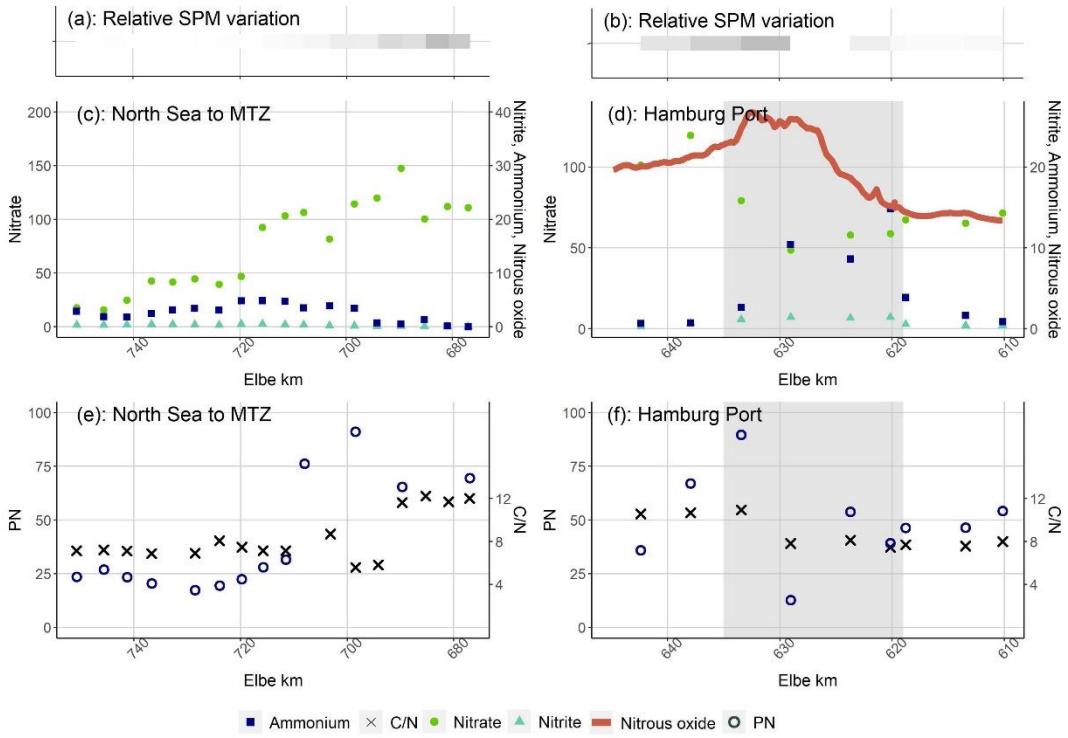

Figure S12: Succession of N-bearing substances coming from the North Sea and in the Port of Hamburg in May 2021: Relative change of SPM concentrations (a) from the North Sea and (b) in the Port of Hamburg. Nitrate in µmol L^{-1}, nitrite in µmol L^{-1}, ammonium in µmol L^{-1} and nitrous oxide concentrations in nmol L^{-1} plotted against stream kilometers (c) from the North Sea and (d) in the Port of Hamburg. Particulate nitrogen concentrations in µmol L^{-1} and C/N values plotted against stream kilometers (e) from the North Sea and (f) in the Port of Hamburg. The grey area in (d) and (f) shows the position of the Port of Hamburg.

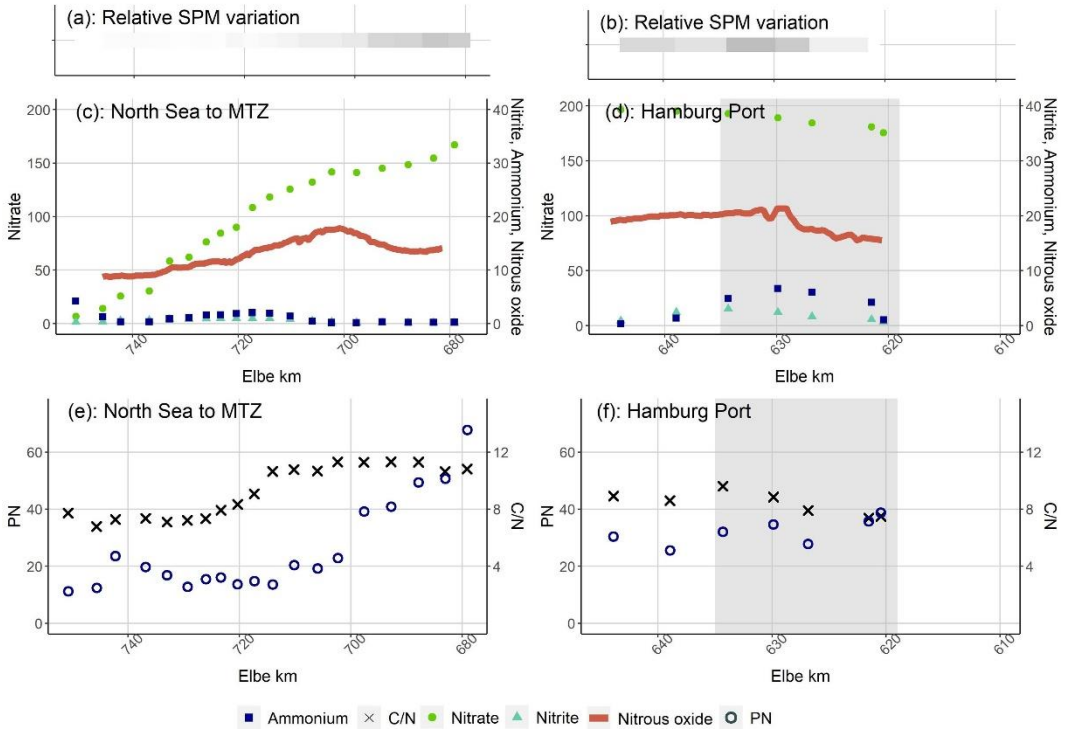

Figure S13: Succession of N-bearing substances coming from the North Sea and in the Port of Hamburg in July 2021: Relative change of SPM concentrations (a) from the North Sea and (b) in the Port of Hamburg. Nitrate in µmol L^{-1}, nitrite in µmol L^{-1}, ammonium in µmol L^{-1} and nitrous oxide concentrations in nmol L^{-1} plotted against stream kilometers (c) from the North Sea and (d) in the Port of Hamburg. Particulate nitrogen concentrations in µmol L^{-1} and C/N values plotted against stream kilometers (e) from the North Sea and (f) in the Port of Hamburg. The grey area in (d) and (f) shows the position of the Port of Hamburg.

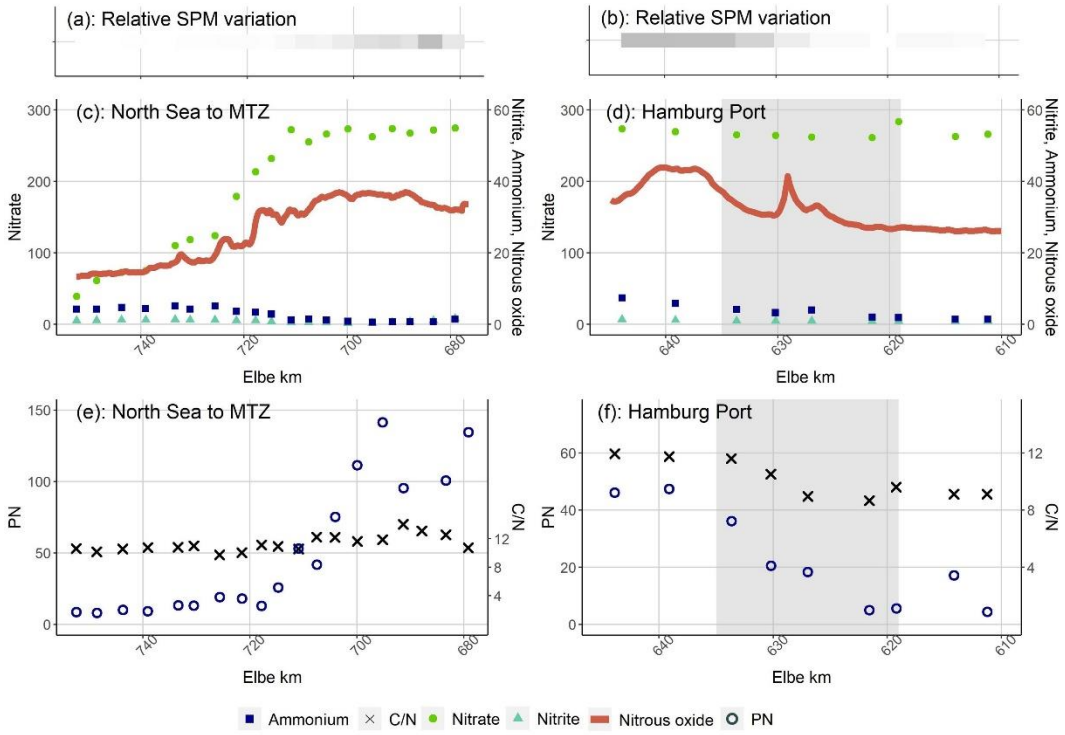

104

105 **Figure S14: Succession of N-bearing substances coming from the North Sea and in the Port of Hamburg in March 2022:**
106 **Relative change of SPM concentrations (a) from the North Sea and (b) in the Port of Hamburg. Nitrate in µmol L^{-1},**
107 **nitrite in µmol L^{-1}, ammonium in µmol L^{-1} and nitrous oxide concentrations in nmol L^{-1} plotted against stream**
108 **kilometers (c) from the North Sea and (d) in the Port of Hamburg. Particulate nitrogen concentrations in µmol L^{-1} and**
109 **C/N values plotted against stream kilometers (e) from the North Sea and (f) in the Port of Hamburg. The grey area in**
110 **(d) and (f) shows the position of the Port of Hamburg.**

111 **References**

112 Clark, J. F., Schlosser, P., Simpson, H. J., Stute, M., Wanninkhof, R., and Ho, D. T.: Relationship between gas
113 transfer velocities and wind speeds in the tidal Hudson River determined by the dual tracer technique, in: Air-
114 Water Gas Transfer, edited by: Jähne, B. and Monahan, E. C., AEON Verlag, Hanau, 785–800, 1995.

115 Das Fachinfomrationssystem (FIS) der FGG Elbe: https://www.elbe-
116 datenportal.de/FisFggElbe/content/start/ZurStartseite.action;jsessionid=A37EDCF5B5EC1ECB15091447E64EC
117 538, last access: 21 November 2022.

118 Pätsch, J. and Lenhart, H.-J.: Daily Loads of Nutrients, Total Alkalinity, Dissolved Inorganic Carbon and
119 Dissolved Organic Carbon of the European Continental Rivers for the Years 1977 – 2009, Institut f¨ur
120 Meereskunde der Universität Hamburg, Hamburg, DE, 2011.

121 Wanninkhof, R.: Relationship between wind speed and gas exchange over the ocean, J. Geophys. Res. Oceans,
122 97, 7373–7382, https://doi.org/10.1029/92JC00188, 1992.